PROC. OF JSCE,
No. 325, Sept. 1982

FATIGUE STRENGTH OF LONGITUDINAL WELDED JOINTS CONTAINING BLOWHOLES

By Chitoshi MIKI, Fumio NISHINO**, Yasuaki HIRABAYASHI*** and Hiroyuki OHGA*****

1. INTRODUCTION

In recent years, partially-penetrated corner welding of single-bevel-groove has come to be often adopted for fabrication of box-section truss members. The current steel railway bridges specification in Japan[1] classified these parts of SS41 to SM58 steels as category A of the design allowable fatigue stresses, and also for the Honshu-Shikoku bridges, which will use up to 800 N/mm^2 class steels, adoption of the same allowable stress had been considered[2]. In 1976 and 1979, the Honshu-Shikoku Bridge Authority conducted large-scale fatigue tests of truss panel point structures of 600 N/mm^2 and 800 N/mm^2 class steels[3),4)], resulting in the corner welds after by far smaller numbers of cycles than expected. It appears that the cause of this failure consist in that lack of fusion remained in the roots for manually welded joints, that blowholes were produced in the roots for submerged arc welded joints and that the fatigue strength were influenced by residual stress. In partially-penetrated single-bevel-groove welds, it may be inevitable to some degree, that irregularities remain at weld metal bottom surfaces and blowhole in the root.

Fisher[5] showed that normal welding procedures for the web-to-flange connections would result in initial discontinuities in the form of porosity, cold laps, slag inclusions and other forms, and discontinuities in such weld connection, that were parallel to the stress field, had no influence on the members' performance. Hirt and Fisher[6] showed that fatigue cracks in the welded beams always originated from discontinuities in the web-to-flange fillet welds such as porosity. Previous study by the authors et al.[7] on partially penetrated longitudinal welds of 800 N/mm^2 class steels clarified that fatigue cracks originated from the irregularities of the weld metal bottom surfaces at weld root at the extremely early stage of the fatigue life.

In the present study, fatigue tests of partially-penetrated longitudinal welded specimens of which roots contain various shapes and sizes of blowholes are carried out to investigate the influences of blowholes on the fatigue strengths of joints. The actual behavior of initiation and propagation of fatigue cracks emanating from blowhole is clarified by the beach mark tests of these specimens. Further, the applicability of fracture mechanics concepts of fatigue crack growth to the prediction of fatigue life of the joints containing blowholes is studied.

2. FABRICATION OF SPECIMENS AND METHOD OF TESTING

(1) Fabrication of Test Plates

The material for testing is 600 N/mm^2 class steel for welded structure SM 58 Q with 16 mm thickness. Its mechanical properties and chemical compositions are shown in **Table 1** according to mill sheet.

Tack welds were done manually and regular welds were done by submerged arc welding. **Tables 2** and **3** show the welding material used and chemical composition of the submerged arc welding wire used.

Fig. 1 shows the configuration of test plate and location of tack welds. The regular weld is prepared by one side-one layer partially-penetrated submerged arc welding while the corner welding of a truss chord member being simulated. The welding condition is shown in **Table 4**.

In order to produce blowholes of various configurations and sizes at the weld roots, following

* Dr. of Eng., Associate Professor, Dept. of Civil Engineering, Tokyo Institute of Technology.
** Ph. D., Dr. of Eng., Professor, Dept. of Civil Engineering, Univeristy of Tokyo.
*** M. Eng., Metropolitan Expressway Public Corporation, (Formerly Graduate Student, University of Tokyo).
**** M. Eng., Research Associate, Tokyo Institute of Technology.

Table 1 Mechanical Properties and Chemical Compositions.

	Tensile Properties			Chemical Composition (%)								
	Y.S. (N/mm^2)	T.S. (N/mm^2)	EL. (%)	C	Si	Mn	P	S	Ni	Cr	V	Ceq
SM58Q (16 mm)	529	627	36	0.14	0.27	1.35	0.017	0.003	0.3	0.2	0.042	0.38

Table 2 Welding Materials.

	Welding Process	Steel	Rod, Wire & Flux	Maker	Rod Size
Tack Welding	Shield metal arc welding	SM58 ×SM58	LB62 (JIS D5826)	KSL	4.0 mmφ
Welding	Submerged arc welding	〃	US49 ×MF38	KSL	4.8 mmφ

Table 3 Chemical Compositions of the Submerged Arc Welding Wire.

Symbol	C	Si	Mn	P	S	Mo
US-49 (4.8 φ)	0.09	0.02	1.58	0.011	0.012	0.52

Table 4 Welding Condition.

Groove	Pre-heating	Welding layer	Current (A)	Voltage (V)	Welding Speed (cm/min)	Heat input (KJ/cm)
Single bevel groove (root gap 0 mm)	50°C	1	700 ~ 720	30 ~ 31	35 ~ 38	Ave. 36

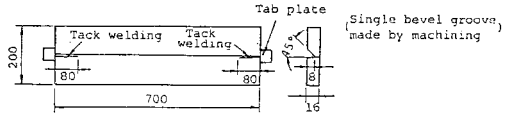

Fig. 1 Configuration of Test Plate and Location of Tack Welding.

four procedures were used for welding the test plates. We investigated various possible execution procedures for poducing blowhole while its size being controlled to some degree, and could gain a prospect of these procedures.

a) Sprinkling water on the plates
b) Spreading wet flux over the plates
c) Spreading red rust or making red rust generate
d) Applying zinc paint on the plate

Radiographic examination of a central 250 mm region of each weld zone were carried out to determine whether blowhole to be generated could be seen or not. The X-ray is photographed with an angle of about 60° to each test plate so that its penetration can be also utilized for estimating approximately the blowhole length.

The test plates were classified as follows on the basis of the breadth of the maximum blowhole measured by radiographic examination in each of them:

no blowhole	Test plate without blowhole
$b \leqq 1$ mm	Test plate with small blowhole
1 mm$<b\leqq$2 mm	Test plate with medium blowhole
2 mm$<b$	Test plate with large blowhole

Most of the test plates which were welded under normal condition contain no blowhole. All test plates which were welded by above mentioned a), b) and c) procedures were classified into the test plates with small blowhole or these with medium blowhole. Most of the test plates which were welded by d) procedure were classified into these large blowhole.

(2) Specimen

The configurations and dimensions of specimens finished from test plate are as shown in

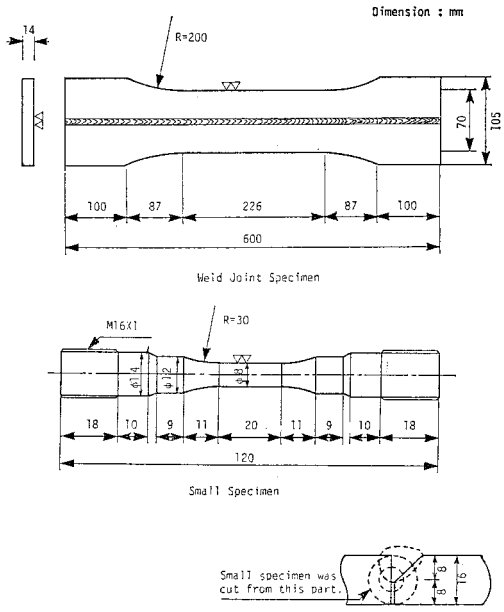

Fig. 2 Configuration and Dimension of Specimens.

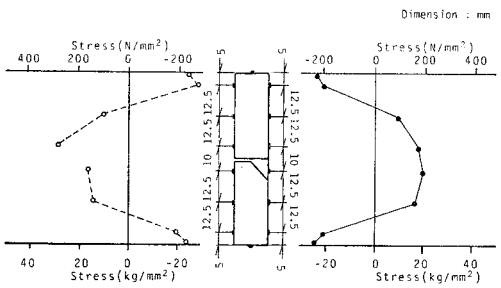

Fig. 3 Welding Residual Stress Distribution of Joint Specimen.

Fig. 2. They consist of joint specimens having parallel portions of 70 mm width and small specimen of $\phi 8$ mm diameter cut out of weld including its root.

Fig. 3 shows the example of welding residual stress distribution of joint specimen measured by stress relief method. Maximum tensile residual stress is about 300 N/mm². The residual stress of small specimen is relieved almost completely.

(3) Performance of Fatigue Test

Fatigue tests of the joint specimens were carried out with two Amsler type fatigue test machines of maximum dynamic loads of 10^3 and 5×10^2 KN, with repeated tension of its minimum value about 20 N/mm² (2 kg/mm²) under a rate of 250 cpm. Fatigue tests of the small specimens were carried out with the electrohydraulic type fatigue test machine of maximum dynamic load 50 KN with repeated tension of its minimum value about 10 N/mm² (1 kg/mm²) under a rate of 600 cpm.

Besides performance of fatigue tests under constant stress range, the fatigue tests under two-stage multistress range were also performed, in which the stress range was reduced to one half every certain number of cycles in order to leave beach marks on the fracture surfaces (beach mark tests).

3. RESULTS OF FATIGUE TESTS

Fig. 4 shows the results of fatigue tests under constant stress range by plotting the stress range S_r on the ordinate and the corresponding failure life N_f on the abscissa, both in logarithmic scale. Each S_r-N_f line is calculated by the method of least squares considering S_r as a random variable of N_f. The 10^6 cycles fatigue strength of each type specimens calculated from S_r-N_f line is shown in figure. Between the fatigue strengths of joint specimen without blowhole and of small specimen, there is a large difference in the same manner as the results described in the previous reports by the authors[7] on the similar type manually welded joints. This fact means residual welding stress remarkably lowers the fatigue strength of joints.

Fatigue test results of all specimens are summarized in **Fig. 5**. Among the welded joint

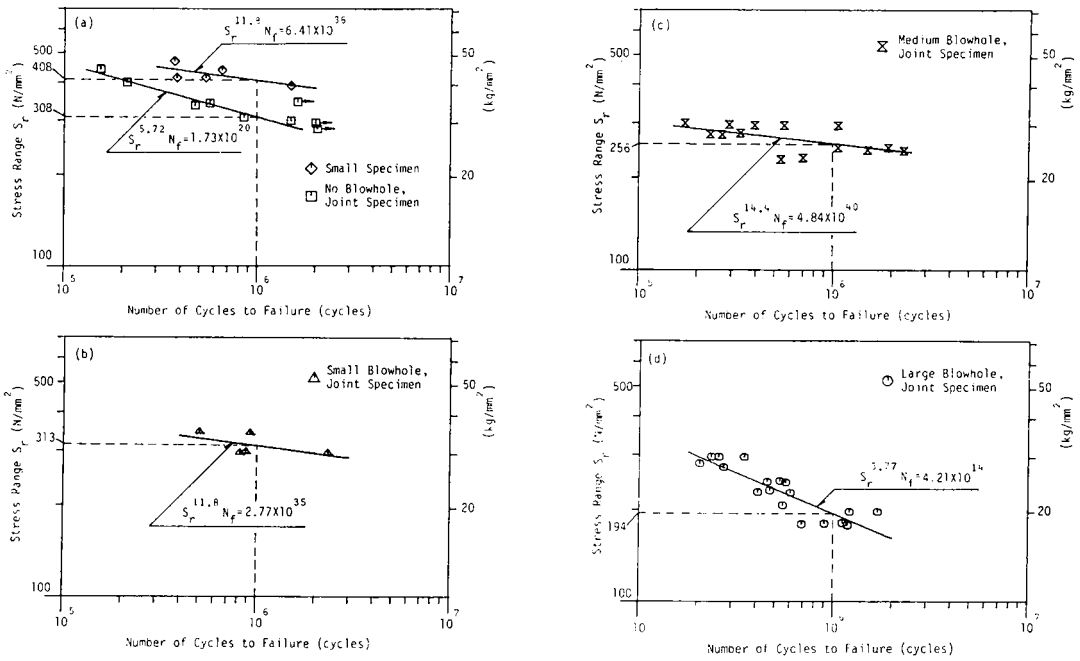

Fig. 4 Results of Fatigue Tests under Constant Stress Range.

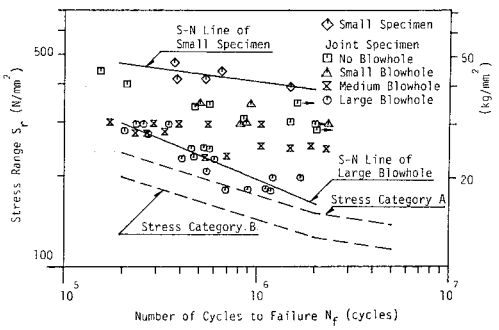

Fig. 5 Summary of Fatigue Test Results.

specimens, the specimen without blowhole and with small blowhole have the same fatigue strength and as the blowoles become larger the fatigue strength remarkably decreases. The reduction in fatigue strength due to existence of medium and large blowhole is substantial and the effect is recognized as being considerably greater than that of the lack of area. The occupation of blowholes in the cross sectional area is less than 0.7%.

The broken lines in **Fig. 5** represent design allowable stress lines for category A and B used for the calculation of cumulative fatigue damage of the Honshu-Shikoku Bridges[2),8)]. The slopes of these lines are 0.2 in the region of N_f less than 2×10^6 cycles and 0.1 in the region of N_f over 2×10^6 cycles respectively. Except one test result, all of the test results are above the design line provided by category A. However, the slopes of design line are considerably gentle in comparison with the test results of large blowhole. The category A design line appears to be unsafe at the region of long fatigue life for this type of weldment in the case of containing large blowhole in it.

After fatigue test, all of the specimens were made to be ruptured along their respective weld lines to observe penetration of the weld metals, the blowholes and fatigue crack initiation. Rupturing was done after thoroughly chilling with liquid nitrogen. **Photo. 1** shows their examples; Radiograph taken after welding and ruptured surface along the weld line are given at the upper and lower photographs respectively. There are plural number of blowholes of similar shapes and sizes in one specimen as shown in the radiographs of **Photo. 1**. Each specimen is failed by the fatigue crack initiated from the blowhole marked with arrow in the radiograph. In most of the joint specimens classified into the large and medium blowholes, fatigue cracks are also initiated from other blowholes different from that on the surfaces of fracture. Even in a part of the joint specimens with small blowhole, it can be confirmed that the plurality of

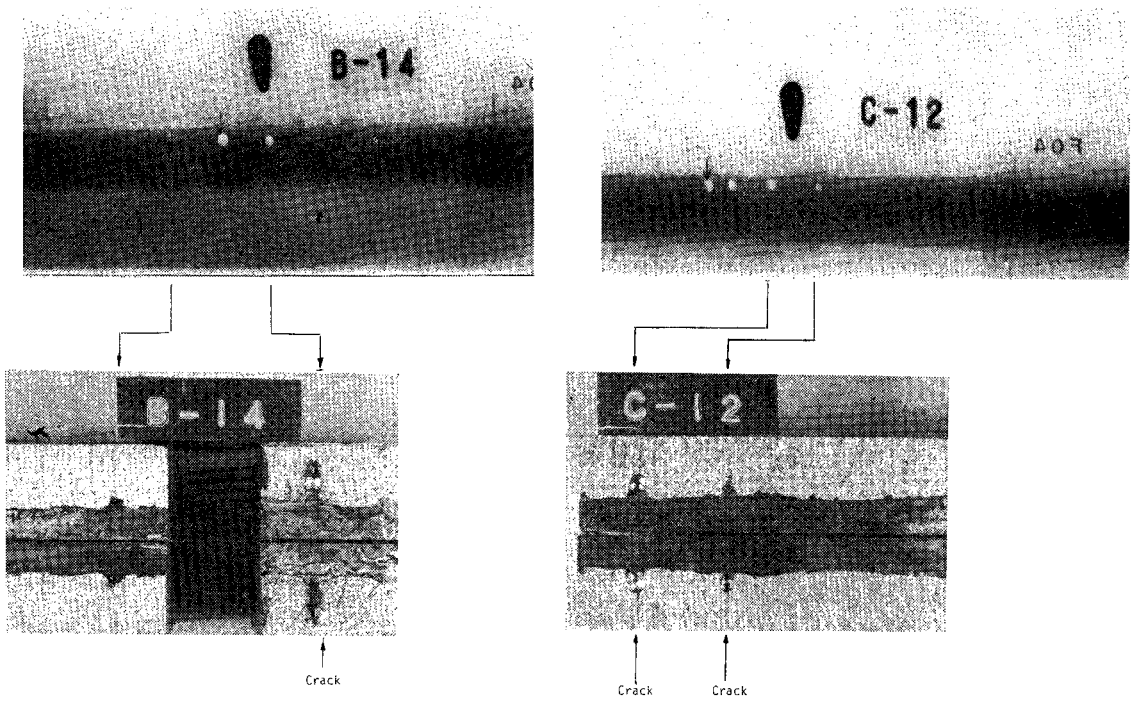

Photo. 1 Fracture Surface along the Weld Line.

fatigue cracks are initiated from some blowholes in one specimen.

4. INITIATION AND PROPAGATION OF FATIGUE CRACK

A beach mark represents the state of fatigue crack at the time of stress condition change. **Table 5** shows the outline of the results of beach mark tests. **Photo. 2** shows the fracture surface with beach marks. **Fig. 6** shows examples of the observation results of beach marks and the stress histories. In **Table 5**, the testing stress ① indicates the larger stress range and the numbers of cycles, ② and ⑥ do not include those corresponding to the stress range reduced to one half. N_c (crack initiation life ⑥) is the number of cycles of testing stress, at which the first beach mark is formed.

In No. 2 specimen, **Fig. 6**, accepted as no blowhole through radiographic examination, the fatigue crack is initiated from a minute blowhole of 0.2 mm in breadth 0.6 mm in length existing in the root. Based on comparative consideration of the number of beach marks to the stress histories, it can be seen that the number of the halving of the total stress range is 17, whereas the first beach mark is formed at the 15th halving of stress range. Consequently, a considerable number of stress repetition is required until fatigue crack initiation. Fatigue cracks initiated from small blowholes in the root portion (2, C-2, 49) circularly propagates to reach the surface.

In No. 4 and No. 40 specimens, which were classified into no blowhole and small blowhole, respectively, no defect exists in the root on the fracture surface and fatigue cracks are initiated from surface flaws due to machining in the root faces. Also in both of these specimens, the crack initiations required considerable numbers on stress repetition.

No. 45 and No. 70 specimens were classified into medium blowhole and No. 77 was classified into small blowhole. In these specimens, fatigue failure are caused by thin pipe-like blowholes at the roots. Several semicircular cracks originate from the wall of a blowhole approximately simultaneously and they are combined into one larger semielliptical crack while growing. The form of the combined crack gradually approaches circule while absorbing the pipe-like blowhole. In each of these three specimens, a small beach mark of 0.3 mm in depth is observed, and N_c/N_f is about 0.44.

In the specimens classified into large blowhole, there exist blowholes of semispindle form, of which vertexes coincide with the respective roots, fatigue cracks originate from their bottom wall. In the B-13 specimens, the number of the halving of the stress range coincides with the number of beach marks left on the fracture surface. Accordingly, this fatigue crack has been already initiated at the first time of the halving of the stress range. In the B-16, C-17 and C-6 specimens 12, 11 and 12 times of the halving of the stress range are performed and 10, 8 and 10 beach marks are left respectively. However,

Table 5 Results of Beach Mark Tests.

Class of Specimen	Specimen No.	Stress Range* kg/mm² (N/mm²) ①	Cycles to Failure** $N_f(\times 10^5)$ ②	Number of Half Stress Range ③	Number of Beach Mark Observed ④	Size of First Beach Mark (mm) ⑤	Cycles of First Beach Mark** $N_c(\times 10^5)$ ⑥	N_c/N_f ⑦
No-Blowhole Welded Joint Specimen	2	35.1 (343)	15.7	17	3	0.5×0.3	11.9	0.76
	4	30.4 (298)	20.0	30	5	2.1×1.2	13.0	0.65
Small-Blowhole Welded Joint Specimen	49	30.5 (299)	8.11	27	13		4.60	0.57
	40***	30.5 (299)	37.5	42				
		35.7 (350)	3.48	3	3	1.4×0.8	0.57	
	77	29.9 (293)	3.41	6	4	0.8×0.3	1.51	0.44
	C-2	30.4 (298)	14.6	36	26		4.00	0.27
Middle-Blowhole Welded Joint Specimen	45	29.7 (291)	5.46	18	10	0.6×0.2	2.40	0.44
	70	24.0 (235)	8.30	15	9	0.2×0.1	3.53	0.43
	90	31.1 (305)	7.19	23	6	3.0×2.0	5.40	0.75
Large-Blowhole Welded Joint Specimen	B-12	18.8 (184)	10.5	18	10	2.7×1.2	4.43	0.42
	B-13	23.7 (232)	2.40	4	4	2.0×1.0	0.50	0.21
	B-16	17.9 (175)	7.30	12	10	1.3×1.6	1.72	0.24
	C- 6	18.6 (182)	6.33	12	10	0.4×0.6	1.48	0.23
	C-17	18.3 (179)	5.73	11	8	1.6×0.6	1.99	0.30

Note: * Test stress range.
** Only cycles of test stress range.
*** No fracture when test stress range was 30.5 (kg/mm²), then change it.

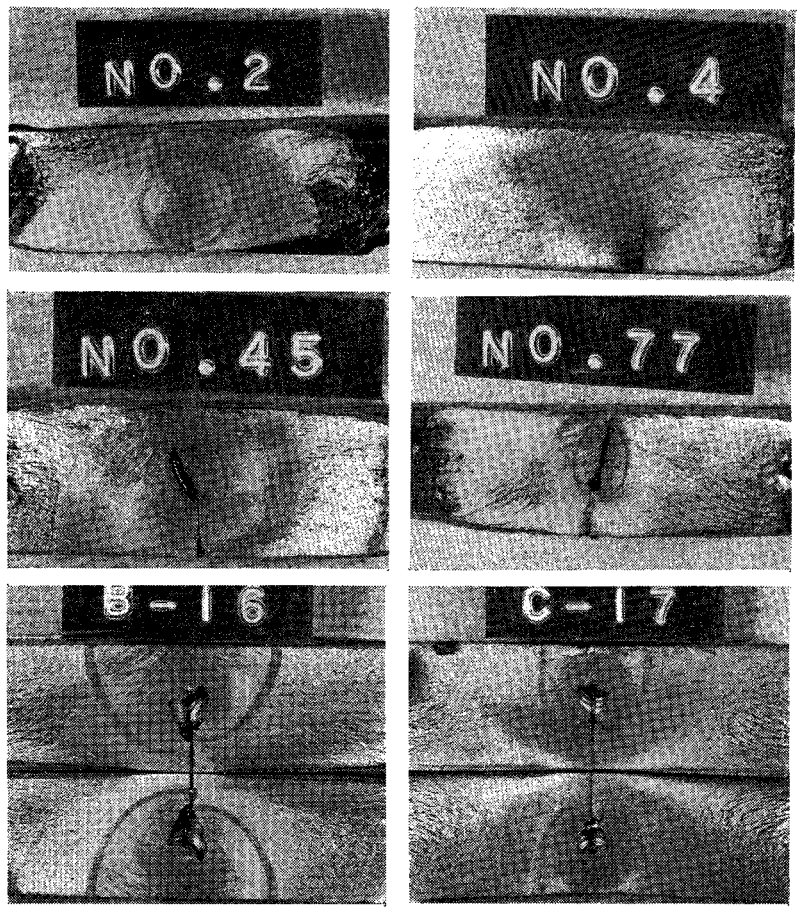

Photo. 2 Fracture Surface with Beach Marks.

because the dimensions of the first beach mark are large, it is thought that 2 or 3 beach marks, which formed inside the first beach mark, have been overlooked in these three specimens. Fatigue cracks initiated from the bottom of large semispindle form blowhole semicircularly propagates along the bottom at early stage and gradually approaches a penny shaped crack to propagate while absorbing the blowhole.

As characteristics of fatigue crack dimension, two quantities (a) and (b) shown in **Fig. 7** are selected and measured. **Fig. 8** shows relationships between the two quantities (a) and (b). Fatigue cracks initiated from small blowholes (2, 49, C-2 specimen) and large semispindle blowholes (B-12, B-13, B-16, C-17 specimen) have roughly $a=b$. Fatigue cracks initiated from a pipe-like blowhole (45, 70, 77 specimen) are combined, at the initial stage, into a temporarily flat semi-elliptic form. However, they are propagated in a manner to be circular.

Fig. 9 shows the dimensions of beach marks (a) of specimens in which small beach marks are observed. The absscissa is taken as "n_t/N_f" (n_t: the number of cycles of testing stress to form individual beach mark) and the ordinate as "a" in logarithmic scale. With specimens containing small blowhole, 75%–85% of failure life are spent for the fatigue crack to propagate to $a=1$ mm. The distance from the location of fatigue crack initiation to the surface of these specimen is about 7 mm, therefore the times at which fatigue crack appears at the surface of specimen are after 95% of failure life. With specimens containing pipe-like blowhole, fatigue cracks of $a=0.1$ mm appear approximately 40% of the failure life. It will be a 70 to 80% of the failure life that the dimension of fatigue crack "a" reaches about 1 mm. With the specimens containing large semispindle blowhole, fatigue cracks are initiated at a very early stage of stress repetition (n_t/N_f are less than 0.2). The time at which fatigue crack appears at the specimen surface are about 90% of failure life.

Let us approximate fatigue crack form with a circle or ellipse, and calculate the stress inten-

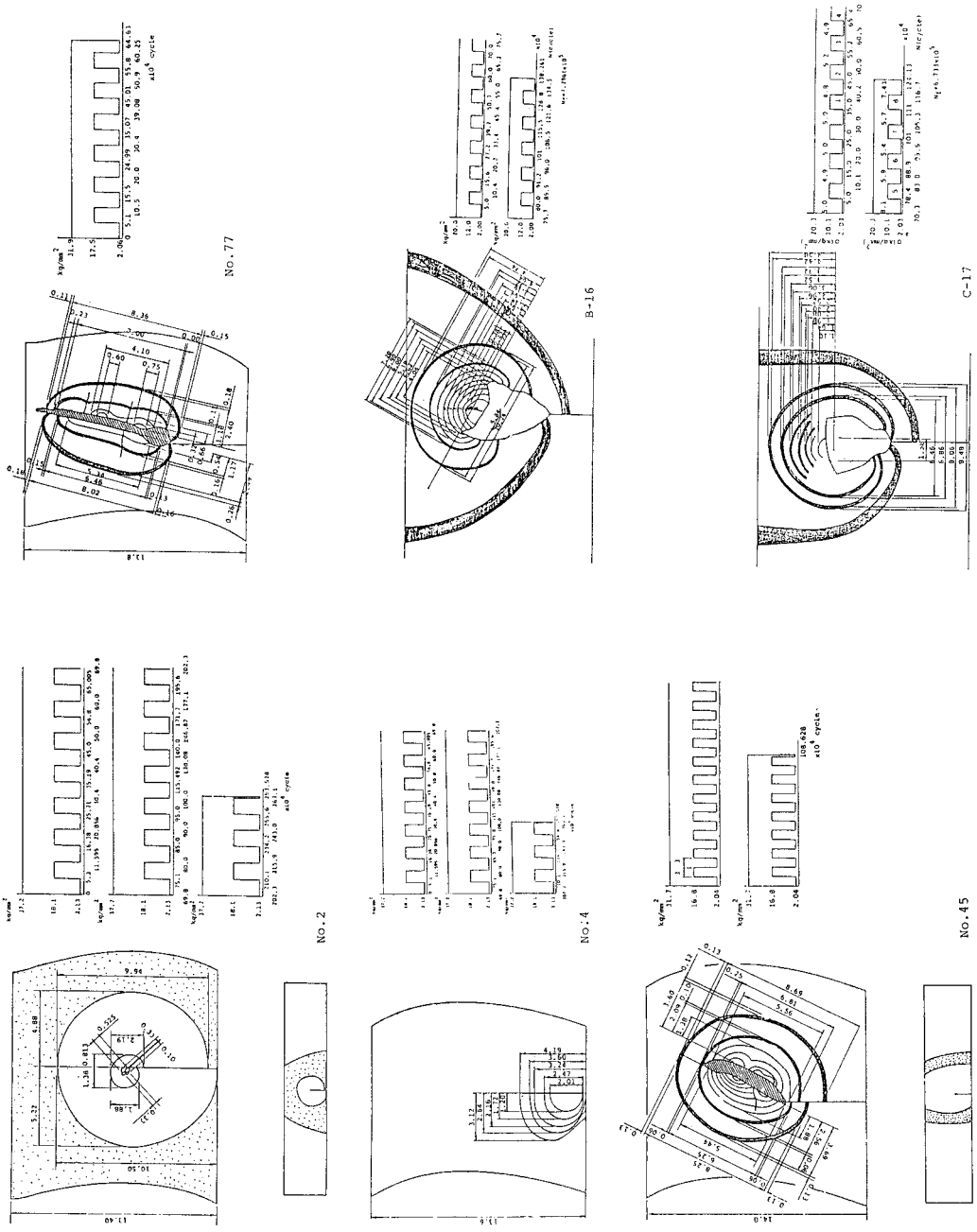

Fig. 6 Sketch of Beach Mark.

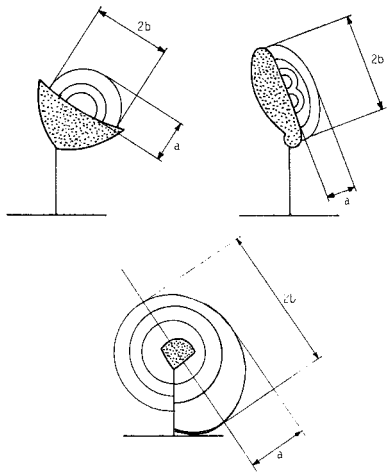

Fig. 7 Dimension of Beach Mark.

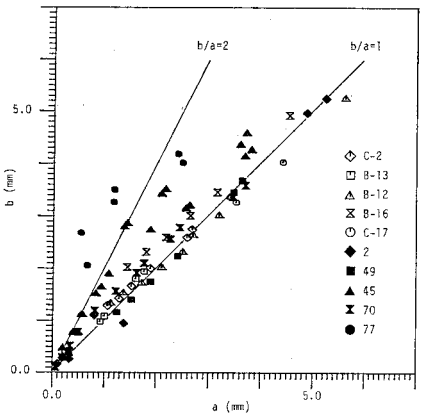

Fig. 8 Configuration of Fatigue Crack.

sity factor range of the fatigue crack from the following equation[9].

$$\Delta K = S_r\sqrt{\frac{\pi a}{Q}}\sec(\pi a/t)(1-0.025\lambda^2+0.06\lambda^4) \quad \cdots\cdots(1)$$

$$Q=\{E(h)\}^2-0.212(S/S_y)^2$$

where

ΔK: Stress intensity factor range
S_r: Stress range
a: Crack depth
Q: Flaw shape parameter
$E(h)$: Complete elliptic integral of the second kind
h: $h^2=1-(a/b)^2$
λ: $2a/t$
t: plate thickness, $t=14$ mm
S: Maximum stress in fatigue test of each specimen
S_y: Yield stress of steel, 529 N/mm²

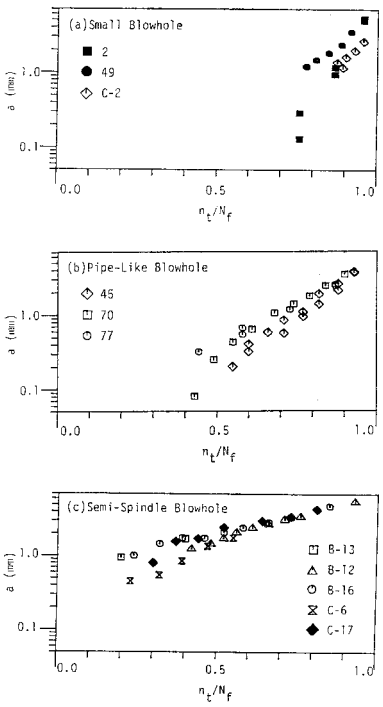

Fig. 9 Fatigue Crack Propagation from Blowhole.

The value of a/b of each fatigue crack is calculated according to **Fig. 7**. The effect of stress concentration by blowhole[10] is not considered in Eq. (1).

Fig. 10 shows a relationship between the fatigue crack growth rate da/dN calculated from the spaces of beach marks and ΔK of each corresponding crack in both logarithmic scales.

Maddox[11] proposed the following equations (2), (3) representing the fatigue crack growth rate in a base metal, C-M_n steel with $S_r=375$ N/mm², weld metal and heat-affected zone of these.

$$\frac{da}{dN}=2.97\times10^{-13}(\Delta K)^{3.0} \quad \cdots\cdots(2)$$

(Upper bound of the growth rate)

$$\frac{da}{dN}=0.90\times10^{-13}(\Delta K)^{3.0} \quad \cdots\cdots(3)$$

(Lower bound of the growth rate)

Okumura[12] and others have arranged the results of fatigue crack propagation tests of 600 N/mm² and 800 N/mm² class steels and welds in Japan and obtained the following relationship as average crack growth rate and stress intensity factor range.

$$\frac{da}{dN}=1.73\times10^{-13}(\Delta K)^{3.0} \quad \cdots\cdots(4)$$

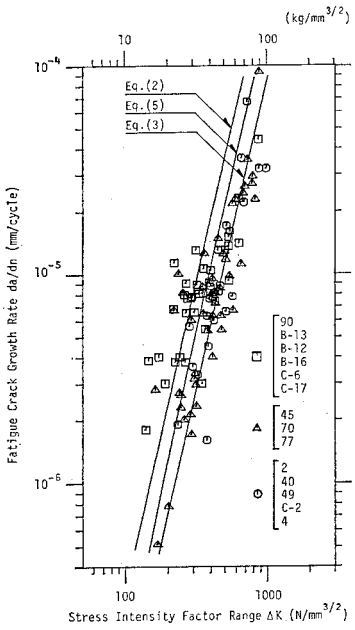

Fig. 10 Fatigue Crack Growth Rate from Beach Mark Spaces.

There is high tensile residual stress in the area where fatigue crack propagates, therefore the threshold stress intensity factor range (ΔK_{th}) is about 78 N/mm$^{3/2}$ [13]. Consequently the fatigue crack growth rate equation considering this ΔK_{th} is obtained from Eq. (4) as shown below.

$$\frac{da}{dN}=1.73\times10^{-13}(\Delta K)^{3.0}-8.34\times10^{-8} \quad \cdots(5)$$

These relationships are shown in **Fig. 10**. Although there are many data which come out of the range restricted by the Maddox's upper and lower bound lines of fatigue crack growth rate, it may said that these fatigue cracks show also the same propagation behavior as that of an ideal two-dimensional cracks in a fatigue crack propagation tests. The line of Eq. (4) is located roughly in the center of these data.

5. ESTIMATION OF FATIGUE CRACK PROPAGATION LIFE

Fatigue crack propagation life (N_p) which is the number of cycles required to propagate a crack from the initial crack size (a_i) to be final crack size (a_f) is estimated based on the following assumptions:

(i) The initial crack at the central part of plate thickness is a penny-shaped crack which simply continues to grow in that shape. Consequently, Eq. (1) is used in which $E(h)$ is equal to $\pi/2$.

(ii) For the relationship between stress intensity factor range and fatigue crack growth rate, Eq. (5) is used.

(iii) The initial crack size (a_i) is to be 0.1, 0.25, 0.5, 1.0, and 2.0 mm.

(iv) The final crack size (a_f) is to be 6.3 mm for all specimens regardless of stress range, because the computed N_p is not sensitive to the a_f. This radius corresponds to 90% of the distance from the location of crack initiation to the surface of specimen.

By substituing Eq. (1) into Eq. (5), fatigue crack propagation life (N_p) can be computed by numerical integration between the two crack sizes a_i and a_f.

Comparison between the estimated S_r-N_p curves and the corresponding experimental values (S_r vs. N_p) is shown in **Fig. 11**. The experimental

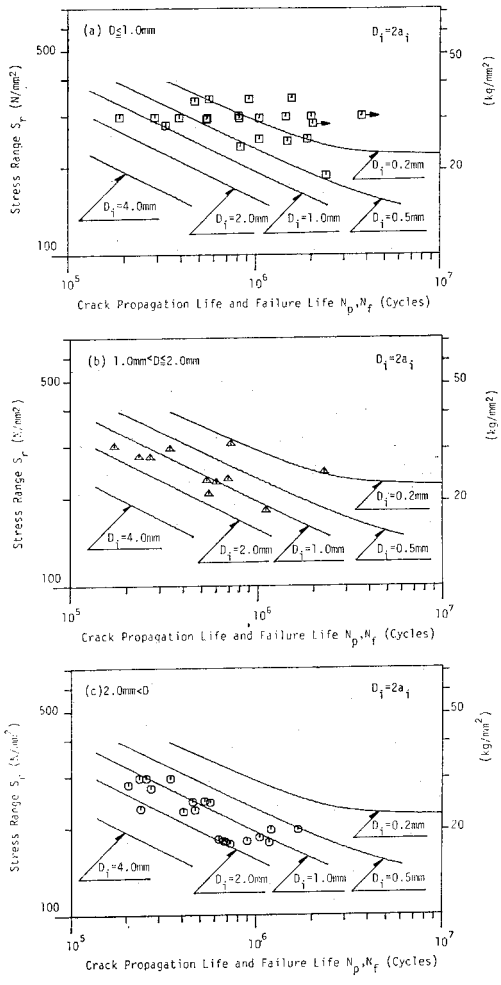

Fig. 11 Comparison between Estimated S_r–N_p Curve and Experimental Values.

values are classified on the basis of the dimension of the circle inscribed in a blowhole measured on fracture surface. As for the crack model for blowhole, Hirt and Fisher[6] used penny-shaped crack with equivalent crack diameter which computed from the equivalence of the K-value with the circumscribed elliptical crack, penny-shaped crack with the diameter of inscribed and circumscribed circle and elliptical crack. From the observation of fatigue propagation through beach mark tests, we consider that inscribed circle is the most appropriate and simplest model. The specimens with no blowhole are included in $D \leqq 1$.

The exprimental values which classified $D \leqq 1$ are widely scattered and most of them go beyond the estimated S_r-N_p curve corresponding to 1.0 mm of D_i $(=2a_i)$ towards the longer lifeside. This is caused by a fact that in the no blowhole specimens and the specimens with minute blowhole considerable number of stress repetition are required before fatigue crack initiation.

Most of the specimens which classified into $1 < D \leqq 2$ contain pipe-like blowholes. These experimental values gather comparatively well in a range between the two estimated S_r-N_p curves corresponding to 1.0 and 2.0 mm of initial crack dimension D_i.

In the all specimens classified into $D > 2.0$, there exist blowholes of semispindle form. These experimental values also gather in a rangebet ween the two estimated S_r-N_p curves corresponding to 1.0 and 2.0 mm of D_i. The results in **Fig. 11** shows that the fatigue strength of longitudinal welded joint containing blowholes can be estimated by fracture mechanics analysis, in which the initial crack is assumed to be a penny-shaped crack of which size is determined as the diameter of the inscribed circle of blowhole for practical convenience.

6. CONCLUSIONS

Partially penetrated longitudinal welded joints in which blowholes were made artificially were tested and their fatigue crack initiation and propagation behavior were investigated. The main conclusions obtained were the following:

(1) There is a large difference between the fatigue strength of joint specimen and of small specimen, which is due to the fact that residual welding stress lowers the fatigue strength. Among the joint specimens, the specimens without blowhole have the highest fatigue strength and as the blowholes become larger the fatigue strength remarkably decreases. The occupation of blowholes in the cross sectional area is less than 0.7%, therefore area diminution by blowholes is negligible.

(2) In the specimens without blowholes and with small blowholes at the root, the crack initiation requires a considerable number of stress repetition. Fatigue cracks initiated from small blowholes in the root portion circularly propagates to reach the surface.

(3) In the specimens with pipe-like blowholes at root, minute semicircular cracks are initiated at several locations of the wall of a blowhole approximately simultaneously and they combined into one larger semielliptical cracks while growing and the form is gradually approaches a penny-shaped to propagate while absorbing pipe-like blowholes.

(4) In the specimens classified into large blowhole, there exist blowholes of semispindle form. Fatigue cracks are initiated from their bottom wall at extremely early stage of the lifes. They semicircularly propagate along the bottom and gradually approaches a penny-shaped to propagate while absorbing blowhole.

(5) In all specimens, fatigue crack appears on the surface only after 90% of its N_f has elapsed.

(6) The experimental values of S_r vs. N_f are classified on the basis of the radius of inscribed circle of blowhole measured on fracture surface. The experimental values of the specimens with pipe-like blowholes and with large semispindle blowholes are close to the corresponding estimated S_r-N_f lines obtained by fracture mechanics analysis on the whole.

ACKNOWLEDGEMENT

This studies were made with guidance and advice from Prof. T. Nishimura of Gunma University. The experimentation work and preparation of paper was done aided greatly by Research Associate T. Sasaki of University of Tokyo. The fabrication of test plate and some part of fatigue tests were done by M. Satoh and K. Yoshida of Mitsubishi Heavy Industries. The authors wish to express their sincerest gratitude to all mentioned above.

REFERENCES

1) Japan Society of Civil Engineers: The Specifications of Steel Railway Bridges, 1974 (in Japanese).
2) Japan Society of Civil Engineers: Fatigue Design for Honshu-Shikoku Bridges, 1974 (in Japanese).
3) Tajima, J., A. Okukawa, M. Sugizaki and H. Takenouchi: Fatigue Tests of Panel Point Structures of Truss made of 80 kg/mm² High

Tensile Strength Steel, IIW., Doc., No. XIII-831-77, July, 1977.

4) Tajima, J., T. Asama, K. Horikawa, Ch. Miki and Y. Kishimoto: Fatigue Strength of Large Size Weldments of High Tensile Strength Steels, International Conference on Welding Research in the 1980's, Osaka University, Japan, Oct. 1980.
5) Fisher, J. W.: Guide to 1974 AASHTO Fatigue Specifications, AISC, May, 1974.
6) Hirt, M. A. and J. W. Fisher: Fatigue Crack Growth in Welded Beams, Engineering Fracture Mechanics, Vol. 5, pp. 415~429, 1973.
7) Nishimura, T., J. Tajima, T. Okukawa and Ch. Miki: Fatigue Strength of Longitudinal Single-Bevel-Groove Welded Members, Proceedings of JSCE. No. 281, pp. 27~40. 1979-11 (in Japanese).
8) Tajima, J., A. Okukawa and Y. Tanaka: Fatigue Design Criteria on Honshu-Shikoku Bridges, 10th Congrress of IABSE, Sept., 1976.
9) Okamura, H.: Guide to Linear Fracture Mechanics, Baifu-kan, May, 1976 (in Japanese).
10) Albrecht, P. and K. Yamada: Rapid Calculation of Stress Intensity Factors, Proc. of ASCE, Vol. 103, No. ST2, 1977.
11) Maddox, S. J.: Assesing the Significance of Flaws in Welds Subject to Fatigue, British Welding Journal, Vol. 53, Research Supplement 401^{s}–409^{s}, Sept. 1974.
12) Okumura, T., T. Nishimura, Ch. Miki and K. Hasegawa: Fatigue Crack Growth Rates in Structural Steels, Proceedings of JSCE, No. 322, pp. 175~178, June 1982.
13) Miki, Ch., F. Nishino, Y. Hirabayashi and K. Takena: Influence of Residual Stress on Fatigue Crack Propagation Rate, Contributed to Proceeding of JSCE.

(Received May 20, 1981)